ACS APPLIED MATERIALS & INTERFACES

RESEARCH ARTICLE

www.acsami.org

Water-Soluble Chitosan-Quantum Dot Hybrid Nanospheres toward Bioimaging and Biolabeling

Ying Lin, Luzhong Zhang, Wei Yao, Hanqing Qian, Dan Ding, Wei Wu, and Xiqun Jiang*

Laboratory of Mesoscopic Chemistry and Department of Polymer Science & Engineering, College of Chemistry & Chemical Engineering, Nanjing University, Nanjing 210093, P. R. China

Jiangsu Provincial Laboratory for Nanotechnology, Nanjing University, Nanjing 210093, P. R. China

Supporting Information

ABSTRACT: A facile approach to prepare CdSe/ZnS quantum dot-encapsulated chitosan hybrid nanospheres (CS-QD) is developed by utilizing ethanol-aided counterion complexation in aqueous solution. The obtained CS-QD hybrid nanospheres have not only the loading space provided by the chitosan spherical matrix for loading multiply QDs but also unique fluorescent properties provided by the encapsulated QDs. Moreover, these hybrid nanospheres possess good biocompatibility and optical stability in physiological environment. It is demonstrated that CS-QD hybrid nanospheres can be internalized by tumor cells and hence act as labeling agent in cell imaging by optical microscopy. In addition, CS-QD hybrid nanospheres can be used for imaging of tumor in tumor-bearing mice via intratumoral administration and can accumulate at tumor site via the blood circulation based on intravenous injection. Thus, on the one hand, chitosan nanospheres provide the protection in both colloidal and optical stability arising from QDs and offer biocompatibility. On the other hand, the encapsulated QDs light up polymer nanospheres and display the fate of polymer nanospheres in cells and bodies.

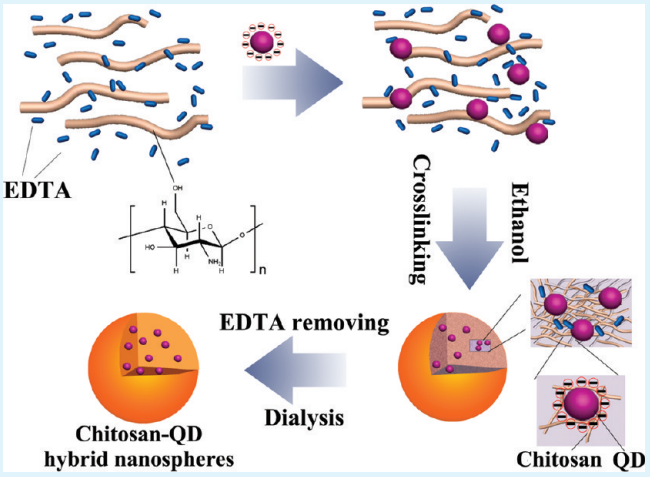

KEYWORDS: chitosan, quantum dots, hybrid nanospheres, imaging

INTRODUCTION

Recently, polymer−inorganic hybrid nanospheres have attracted increasing attention because of the synergic properties arising from both the polymeric nanospheres and inorganic nanomaterials.[1−11] Especially those that are biocompatible and able to emit fluorescence are greatly useful in monitoring nanosphere journey in cell and body, detecting disease sites and reporting therapy response. Compared with organic fluorescent dyes, the inorganic fluorescence-emitters such as quantum dots (QDs) exhibit more robust fluorescence intensity, greater photostablility, a broader excitation wavelength range, and a narrower emission spectrum.[11] Therefore, extensive studies have concentrated on utility of QDs as imaging agents for multicolor imaging cells, tissues, and animals.[7−10,12−17] However, the biomedical and clinical applications of QDs are limited by their poor biocompatibility and instability in different physiological environments. Many strategies are being developed to overcome these limitations. The most successful approach has been to coat QDs with biocompatible water-soluble polymers, which increases QDs colloid stability in aqueous solution and biological milieu, and improves their biocompatibility.[6,8] However, such thin polymer layer at the surface of QDs is difficult to meet the demand to carry enough active molecules. On the other hand, enwrapping QDs with biocompatible polymer nanospheres to replace thin polymer layer will provide enough space for the loading of other active agents such as drugs (see Figure S1 in the Supporting Information) and inorganic nanoparticles, which can extend their application into areas like disease therapy and diagnosis, making them becomes multifunctional nanodevices. In turn, fluorescence-emitting QDs will report the trace and fate of polymer nanocarries in cells and body, exerting their labeling role. In addition, QDs in polymer matrix may diminish QD shell shedding that commonly leads to photodegradation.[6] However, the most construction of QD-associated polymer nanocarriers reported so far require complicated synthesis processes and may cause environmental toxicity, which arise from either the use of surfactants or the organic solvents. Moreover, some of QD

Received: October 11, 2010
Accepted: February 23, 2011
Published: March 09, 2011

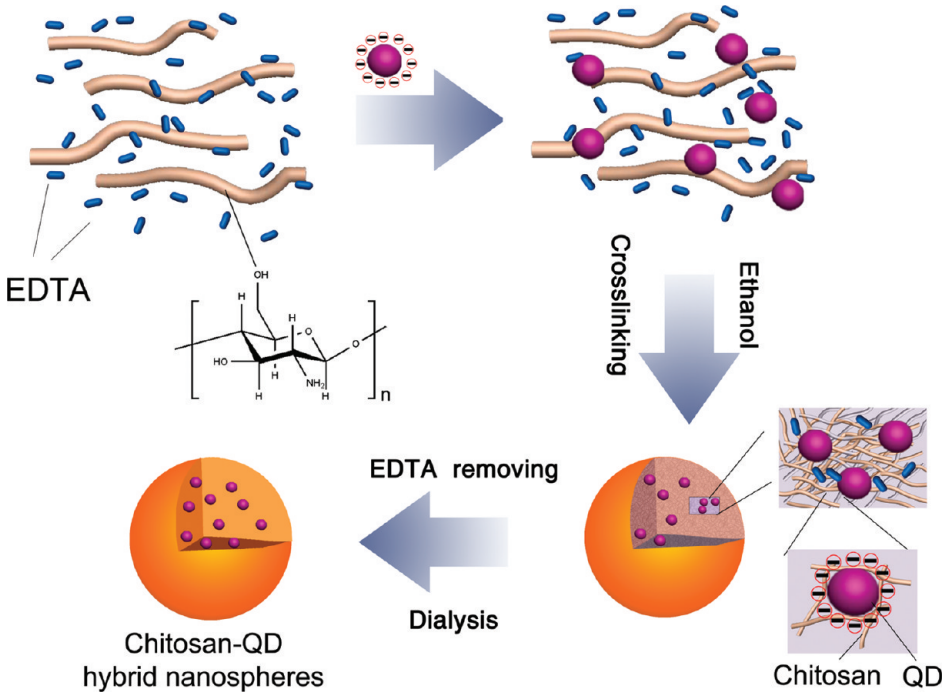

Figure 1. Schematic illustration of the preparation of CS-QD hybrid nanospheres.

encapsulations with polymers often cause the disappearance in QD fluorescence intensity.[18]

Chitosan (CS) is a linear natural polysaccharide composed of β-(1→4)-2-amido-2-deoxy-D-glucan (glucosamine) and β-(1→4)-2-acetamido-2-deoxy-D-glucan (acetyl glucosamine) units, and prepared from N-deacetylation of chitin extracted from crustacean shells. Because of its good biocompatible, biodegradable, and low-toxicity properties, chitosan has been widely used in biomedical field as a carrier for drugs or other biomaterials.[4,19] Chitosan is also a cationic polyelectrolyte which will enhance the cellular binding and internalization of QD for ex vivo cell labeling. Although there are several works about QD/chitosan systems,[20,21] the stability of these systems in physiological environments remains substantial challenges.

Herein, we report a facile approach to the fabrication of chitosan-QD hybrid nanospheres based on low-molecular-weight, water-soluble CS and CdSe/ZnS QDs as schematically shown in Figure 1. The resultant CS-QD hybrid nanospheres embedding multiple QDs not only are stable in aqueous solution and physiological environment but also retain their fluorescent characteristics. The ability of biological imaging and labeling of the CS-QD hybrid nanospheres in vitro and in vivo were evaluated. In vivo fluorescent imaging in tumor-bearing mice indicates that the fluorescence from QDs of hybrid nanospheres can be visualized in tumor. Moreover, the chitosan-QD hybrid nanospheres enhance QDs retention within solid tumor.

EXPERIMENTAL SECTION

Materials. Chitosan (CS) with number-average molecular weight (Mn) of 5000 was purchased from Yuhuan Biomedical Company (Zhejiang, China) and used without further purification. Cadmium oxide (CdO), hexamethyldisilathiane ($(TMS)_2S$), diethylzinc ($Zn(Et)_2$), trioctylphosphine oxide (TOPO), trioctylphosphine (TOP), Ethylene diamine tetraacetic acid (EDTA) and glutaraldehyde (GA) were purchased from Aldrich. Hexadecylamine (HDA), selenium, 3-mercaptopropionic acid (3-MPA) and stearic acid are products of Alfa Aesar. All chemicals were used as received. All other ingredients were analytical grade unless otherwise stated.

Synthesis of CdSe/ZnS QDs. Luminescent CdSe/ZnS QDs were synthesized following the procedures reported previously,[22,23] with minor modifications. Briefly, 12.7 mg of CdO and 114 mg of stearic acid were added into a 100 mL three-neck flask and heated to 150 °C under Ar flow. After CdO was completely dissolved, 1.94 g of TOPO and 1.94 g of HDA were added to the flask. Then, the mixture was heated to 280 °C under an Ar flow. At this temperature, 2 mL of a TOP solution containing 79 mg of selenium was swiftly injected into the reaction system under vigorous stirring. The color of the reaction mixture changed from colorless to yellow, orange, or red within 1 min. Subsequently, the temperature of the solution was cooled to 200 °C, a solution containing 100 μL ($(TMS)_2S$) and 370 μL ($Zn(Et)_2$) premixed in 2 mL of TOP was gradually injected into the flask over 3 min. The reaction system was kept at 180 °C and stirred for 40 min. Finally, the reaction system was cooled to 90 °C and stirred for one hour. The mixture was diluted by 15 mL of chloroform. The resulting sample of CdSe/ZnS QDs was precipitated by adding methanol into the solution, collected by centrifugation, and redispersed to chloroform. The concentration of resulting QDs solution was calculated based on a method developed by Peng et al,[24] the concentration of CdSe core solution was first calculated, and then the concentration of CdSe/ZnS QDs solution was determined.

Preparation of CS-QD Hybrid Nanospheres. The CS-QD hybrid nanospheres were synthesized by a non-solvent-aided counterion complexation method. First, 25 mg of CS was dissolved in 8 mL of deionized water. A predetermined amount of EDTA was then added to the CS aqueous solution and stirred until the EDTA fully dissolved. The as-prepared QDs were transferred from chloroform into deionized water with the aid of 3-MPA according to reported procedures.[25] 4.2 nmol of water-soluble QDs were precipitated by ethanol, centrifuged, redispersed to deionized water twice, and then added subsequently to the CS-EDTA mixture solution. The resultant mixture was stirred for 2−3 min. After that, ethanol, a nonsolvent for both chitosan and EDTA, was added

dropwise to the system under stirring until the clear solution turned opalescent, which indicated the formation of CS-EDTA colloidal particles and QDs were spontaneously encapsulated into CS-EDTA colloidal particles. Eleven microliters of GA aqueous solution (25%) was then added into the colloidal solution to cross-link CS of obtained hybrid nanospheres and the cross-linking reaction was allowed to proceed for 2 h at room temperature. The obtained suspension was filtrated and pH of suspension was adjusted using 2 M ammonia solution to pH = 10.0. After that, the suspension solution was centrifugated and the sediment was redispersed into deionized water. Finally, the particle solution was dialyzed against deionized water at pH = 9 for 24 h to remove EDTA component in the particles to obtain CS-QD hybrid nanospheres.

Characterization of QDs and CS-QD Hybrid Nanospheres. Photoluminescence (PL) spectra were taken with RF-5301PC spectrofluorometer (Shimadzu, Japan), and UV−vis absorption spectra were collected using UV3100 spectrophotometer (Shimadzu, Japan). Slit width of the spectrofluorometer was 5 nm in both the excitation and emission monochromators. Samples were placed in an open-sided, 1 cm path length quartz cuvette for both PL and UV−vis measurements. Fluorescence quantum yields were estimated by comparing the integrated fluorescence intensity of the sample solutions and rhodamine B in matched absorbance region. Samples were diluted so that they were optically thin. X-ray powder diffraction patterns of the samples were collected on a Shimadzu XRD-6000 Diffractormeter using the Cu−Kα radiation. Morphological studies of the hybrid nanospheres were carried out using high-resolution transmission electron microscopy (HRTEM) (JEM-2100, JEOL), scanning electron microscopy (SEM) (S-4800, Hitachi). For HRTEM observations, the specimens were prepared by drop-coating the sample dispersion onto an amorphous carbon-coated 300 mesh copper grid. A drop of the suspension was placed on a clean silicon wafer and air-dried for SEM observations. The mean diameter, size distribution and zeta potentials of the prepared nanospheres were determined by a dynamic light scattering (DLS) method using a Brookhaven BI-9000AT instrument and a Zetaplus (Brookhaven Instruments Corporation), respectively. All results were the average of triplicate measurements.

QD Encapsulation Efficiency. The CS-QD hybrid nanospheres stock solution was centrifuged and the sediment was lyophilized. Freeze-dried hybrid nanospheres were weighted and then were analyzed by thermogravimetry analyses (TGA). TGA were performed using TAC71DX thermal analyzer under N_2 flow in the temperature range 25−800 °C at a heating rate of 20 °C/min. The amount of free QDs in the supernatant was quantified using inductively coupled plasma atomic emission spectroscopy (ICP-AES) (J-A1100, Jarrell-Ash). QDs encapsulation efficiency was calculated with the following equation

$$\text{encapsulation efficiency}\% = \frac{\text{weight of QDs in the hybrid nanospheres}}{\text{weight of the feeding QDs}} \times 100\%$$

Cytotoxicity Assays. Cytotoxicity of the CS-QD hybrid nanosphere was evaluated by 3-(4,5-dimethylthiazole-2-yl)-2,5-diphenyltetrazolium chloride (MTT) assays. HeLa cells were seeded into a 96-well plate at a density of 5000 cells per well and incubated at 37 °C in humidified atmosphere with 5% CO_2. The culture medium was a Dulbecco's modified Eagle's medium (DMEM, Gibco) supplemented with 10% fetal bovine serum (FBS, Hyclone, Logan, UT), streptomycin at 100 ug/mL, penicillin at 100 U/mL, 4 mM L-glutamine and changed every other day until 80% confluence had been reached. The medium was then replaced with 100 μL of a medium containing CS nanospheres and CS-QD hybrid nanosphere solution with different concentrations. One row of the 96-well plates was used as control. After incubation for 24 h, 20 μL of a 5 mg/mL MTT solution was added to each well, and the plate was incubated for 4 h, allowing the viable cells to reduce the yellow MTT to dark-blue formazan crystals, which were dissolved in 150 μL of dimethyl sulphoxide (DMSO). The absorbance of individual wells was measured at 570 nm by an ELISA reader (Huadong, DG-5031, Nanjing). The cell viability was determined by following equation:

$$\text{cell viability}\% = \frac{\text{absorbance test cells}}{\text{absorbance controlled cells}} \times 100\%$$

Confocal Laser Scanning Microscopy (CLSM). The CS-QD hybrid nanospheres were incubated with Hela cells for 4 h. Then these cells were washed three times with cold (4 °C) and warm (37 °C) PBS, successively. After that, the cells were observed with a confocal system (Zeiss LSM 710, Germany) by the red channels. The samples were excited at 488 nm.

Small Animal Imaging Studies. Six to seven week old ICR mice (20−25 g) were purchased from Laboratory Animal Center of Nanjing Medical University. H_{22} tumor cells ($5-6 \times 10^6$ cells/mouse) were inoculated subcutaneously to animals at the left axilla. Tumor growth was monitored daily until it reached the acceptable sizes. The mice were divided into two groups for intratumoral and tail vein injection study, respectively. On the one hand, the mice were administered CS-QD hybrid nanospheres (equivalent to 50 pmol of QD) by intratumoral injection and anesthetized with isoflurane at various time points post-injection. The sedated animals were then imaged using the Maestro in vivo optical imaging system (CRI, Inc., Woburn, MA). On the other hand, CS-QD hybrid nanospheres (equivalent to 50 pmol of QD) were injected into H_{22} tumor bearing mice through a tail veil. Then the mice were killed and tumor tissue was harvested for isolated organ imaging at 24 h post i.v. administration.

RESULTS AND DISCUSSION

Preparation of CS-QD Hybrid Nanospheres. To synthesize CS-QD hybrid nanospheres, CdSe/ZnS QDs with excellent fluorescence characteristics were first prepared. Here, CdSe/ZnS QDs with the emission wavelength at around 620 nm was obtained by solution-phase synthesis for reducing autofluorescence from animal tissues and increasing penetration depth of excitation light as full steam.[26] TOPO and HDA were used to passivate the CdSe/ZnS QDs surfaces, thereby rendering them dispersible in chloroform. For construction of CS-QD hybrid nanospheres in aqueous solution, the as-prepared QDs were transferred from chloroform into deionized water with the aid of 3-MPA by surface ligand exchange. The fluorescence quantum yield (QY) of the water-soluble and 3-MPA-coated CdSe/ZnS QDs is about 38.9% of the original value (86.4% in chloroform).

CS-QD hybrid nanospheres were synthesized by a nonsolvent-aided counterion complexation method, as schematically shown in Figure 1, using water-soluble CdSe/ZnS QDs, EDTA, and low-molecular-weight chitosan as the starting materials. The 3-MPA-coated CdSe/ZnS QDs were initially dispersed in an aqueous solution containing chitosan and EDTA. Thus, cationic chitosan should undergo counterion condensation with multivalent anionic EDTA and negatively charged CdSe/ZnS QDs in aqueous solution, to form colloidal aggregates. However, because of the excellent water-solubility of chitosan with low molecular weight, the water-insoluble counterion complexes between chitosan and EDTA as well as CdSe/ZnS QDs did not occur. Therefore, ethanol, a nonsolvent for QDs, chitosan and EDTA, was added to the aqueous solution to facilitate counterion interactions between the positively charged chitosan chains and the anionic EDTA as well as negatively charged CdSe/ZnS

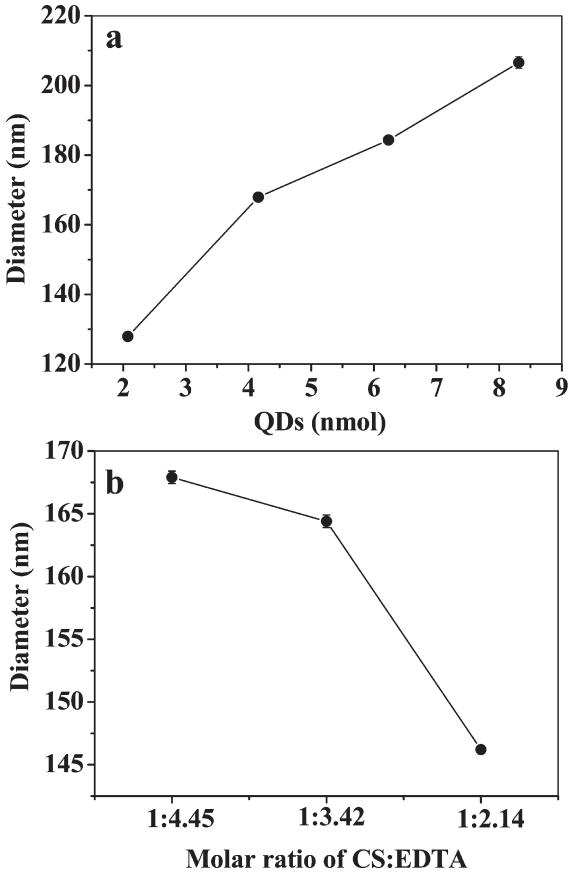

Figure 2. (a) Mean hydrodynamic diameters of CS-QD hybrid nanospheres prepared with different quantity of QDs added, and (b) molar ratios of CS to EDTA.

QDs to form CS-EDTA-QDs nanospheres. Consequently, CdSe/ZnS QDs were effectively encapsulated within the chitosan-EDTA spheres. After the chitosan moiety of the nanospheres was cross-linked by glutaraldehyde, EDTA, a building block of the nanospheres, was removed by dialysis against basic water because of its small molecule character, while CdSe/ZnS QDs were left inside the cross-linked chitosan spheres. Thus, the CS-QDs hybrid nanospheres with cationic chitosan matrix and CdSe/ZnS QDs were obtained.

To optimize our synthesis parameters, various ratios of EDTA, CS, and QDs were utilized to prepare CS-QDs hybrid nanospheres. First, with a constant ratio of EDTA and CS (4.45:1 molar ratio), the hybrid nanospheres were synthesized by changing the amount of QDs added in the system and monitored by DLS. As shown in Figure 2a, the hydrodynamic diameter of CS-QDs hybrid nanospheres increases from 127.9 to 206.6 nm with the increasing QDs added from 2.07 nmol to 8.3 nmol. As mentioned earlier, the negatively charged QDs play a counterion role similar as EDTA in the formation of CS-QD hybrid nanospheres. In addition, as presented in Figure 2(b), the size of CS-QD hybrid nanospheres decreases slightly from 167.9 to 146.2 nm with changing the molar ratio of CS to EDTA from 1:4.45 to 1:2.14. Apparently, these particle sizes are well suitable for efficient transportation and against rapid clearance in vivo.[27,28] Also, both results suggest that the size of nanospheres decreases with decreasing negatively charged moiety since hydrophobic (charge-neutral) moieties decrease. Although a higher loading

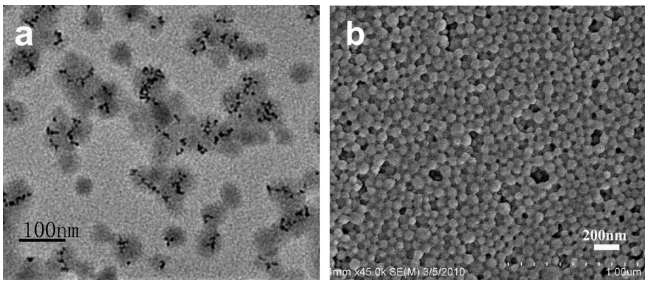

Figure 3. (a) TEM image of CS-QD hybrid nanospheres. (b) SEM image of CS-QD hybrid nanospheres.

level of QDs could endow each CS-QD hybrid nanosphere with more prominent photoluminescence properties, it also compromises the dispersion stability of hybrid nanospheres. When the QDs amount adding in system was up to 8.3 nmol, the irreversible agglomeration of the CS-QD hybrid nanospheres occurred during store. Therefore, in subsequent experiments, to achieve a good balance between the nanosphere stability and photoluminescence intensity of each nanosphere, the CS-QD hybrid nanospheres prepared with 4.2 nmol QDs added were used. The QD encapsulation efficiency was about 92% for these CS-QD hybrid nanospheres.

Figure 3 shows the TEM and SEM images of CS-QD hybrid nanospheres. From TEM image, it can be seen that the CS-QD hybrid nanospheres have a spherical outline and uniform size. The sphere size observed under TEM is smaller than the DLS result due to the shrinking in dry state. The markedly high electron density of QDs enables the direct visualization of the QDs within CS nanospheres. It is found that all of QDs are enwrapped into CS nanospheres and most of CS nanospheres contain the multiply QDs although minority CS spheres are empty. The average encapsulation number of QDs in each CS nanosphere is about 9 based on the TEM images. SEM observation shown in Figure 3b further confirms the spherical structure in shape for CS-QD hybrid nanospheres, and the size is consistent with that in TEM observation. These results suggest that the QDs encapsulation method based on the nonsolvent aided counterion complexation between cationic CS and anionic EDTA and 3-MPA-coated CdSe/ZnS QDs works well.

Fluorescence Properties of CS-QD Hybrid Nanospheres. In contrast to aggregation and the photoinstability of the water-soluble QDs, which are two major barriers for QDs used as biological probes,[6,25] QDs inside chitosan nanospheres exhibit significant photoluminescence stability, because of the effective protection of QDs with thick polymer matrices. Figure 4a presents the UV absorption and photoluminescence spectra from water-solution QDs and CS-QD hybrid nanospheres, as well as photoluminescence spectra of empty CS nanospheres. It has been observed that after chitosan matrix encapsulation, the CS-QD hybrid nanospheres retain the similar shape and same peak position as the unencapsulated QDs except of the peaks caused by the scattering of chitosan nanospheres. Therefore, the optical properties of the QDs are unchanged after encapsulated. In addition, the peak position of the CS-QD hybrid nanospheres is the same as the empty chitosan nanospheres in the wavelengths less than 580 nm. Figure 4b shows the effect of medium pH for the CS-QD hybrid nanospheres on the fluorescence spectra. It can be seen that the fluorescence intensity of CS-QD hybrid nanospheres becomes stronger and stronger when medium pH

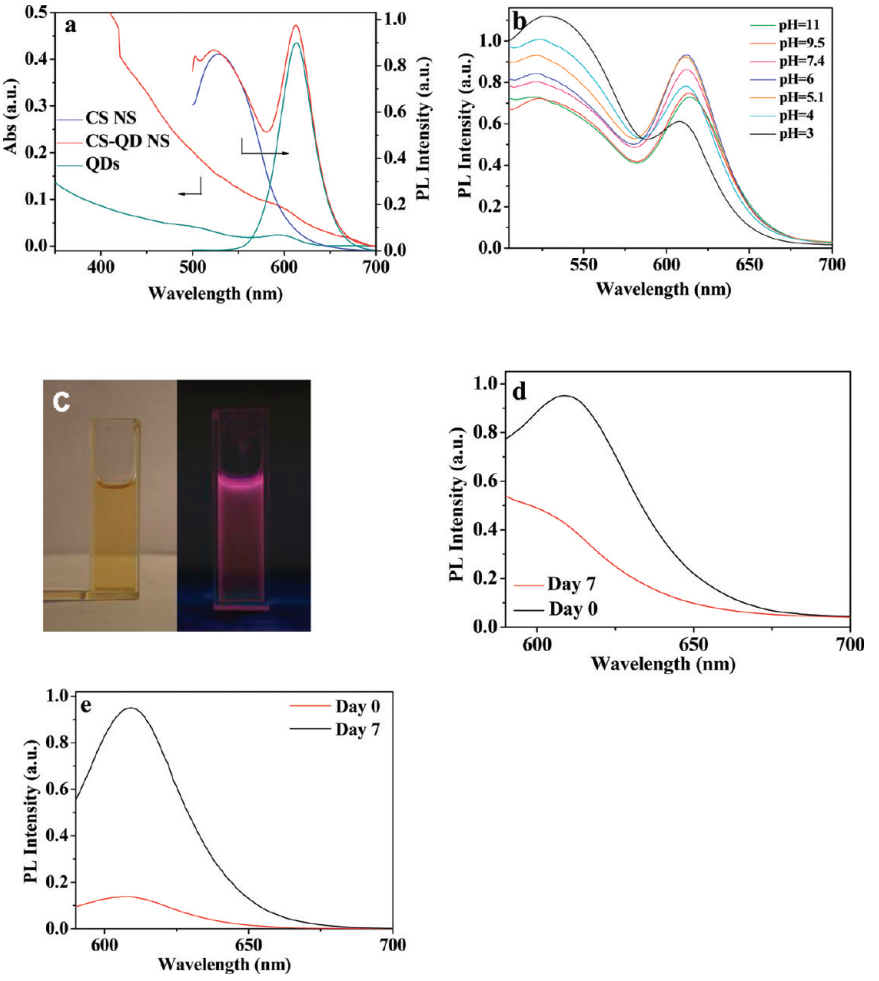

Figure 4. (a) UV−vis absorption and PL spectra of 3-MPA-coateded QDs (dark cyan) and CS-QD hybrid nanospheres (red), and fluorescence emission spectrum of empty CS nanospheres (blue), λ_{ex} = 480 nm. (b) Fluorescence emission spectra of CS-QD hybrid nanospheres dispersed in aqueous solution at different pH values, λ_{ex} = 480 nm. (c) Photographs of CS-QD hybrid nanospheres in aqueous solution with pH = 7.4 under daylight (left) and UV light irradiation (right). (d) PL spectra of the CS-QD hybrid nanospheres in aqueous solution at physiological pH (7.4) over a week at room temperature. (e) PL spectra of 3-MPA-coated QDs in aqueous solution at physiological pH (7.4) over a week at room temperature.

increases from 4 to 6, and reaches maximum at pH 6, which is well-suited for the detection of tumors because the tumor microenvironment is weakly acidic. Continuously increasing pH, the fluorescence intensity of CS-QD hybrid nanospheres turnovers to decrease and becomes quite weak at medium pH 11. It has been demonstrated in suitable acidic range that the shell of Zn^{2+}-MPA complexes on the CdSe/ZnS core would be produced, which tightly covers the surface of CdSe/ZnS QDs and removes the surface trap sites of QDs.[29,30] In addition, the fluorescence intensity of QDs will decreases with increasing the surface trap sites of the QDs. Thus, at pH = 6, the stronger fluorescence signal of CS-QD hybrid nanospheres is probably due to the overlay of Zn^{2+}−MPA complexes, which decreases the surface trap sites of CdSe/ZnS QDs. In other words, when pH is below 4 or beyond 7.4, the dissociation of Zn^{2+}−MPA complexes led to the increase in the surface trap sites of QDs and the sharp decrease in fluorescence intensity of QDs. Moreover, the emission peak position of CS-QD hybrid nanospheres had a slight blue shift within 6 nm when medium pH decreases from 11.1 to 3.

Figure 4c displays the fluorescence photograph of CS-QD hybrid nanospheres. The bright photoluminescence was clearly observed under UV irradiation. Also, the fluorescence of hybrid nanospheres dispersed in PBS (pH 7.4) could be retained over a

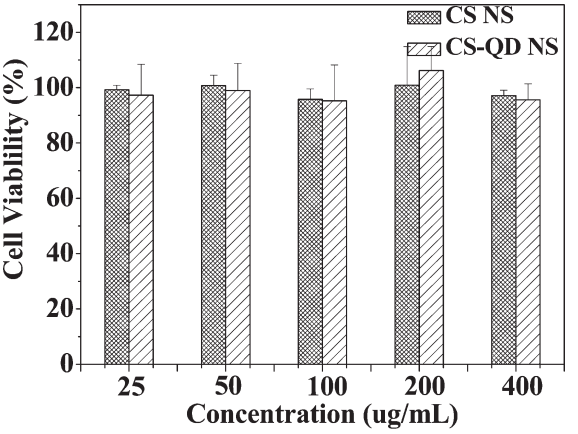

Figure 5. Viability of HeLa cells incubated with as-prepared empty chitosan nanospheres (CS NS) and CS-QD hybrid nanospheres (CS-QDs NS) at different concentrations.

dx.doi.org/10.1021/am100982p |ACS Appl. Mater. Interfaces 2011, 3, 995–1002

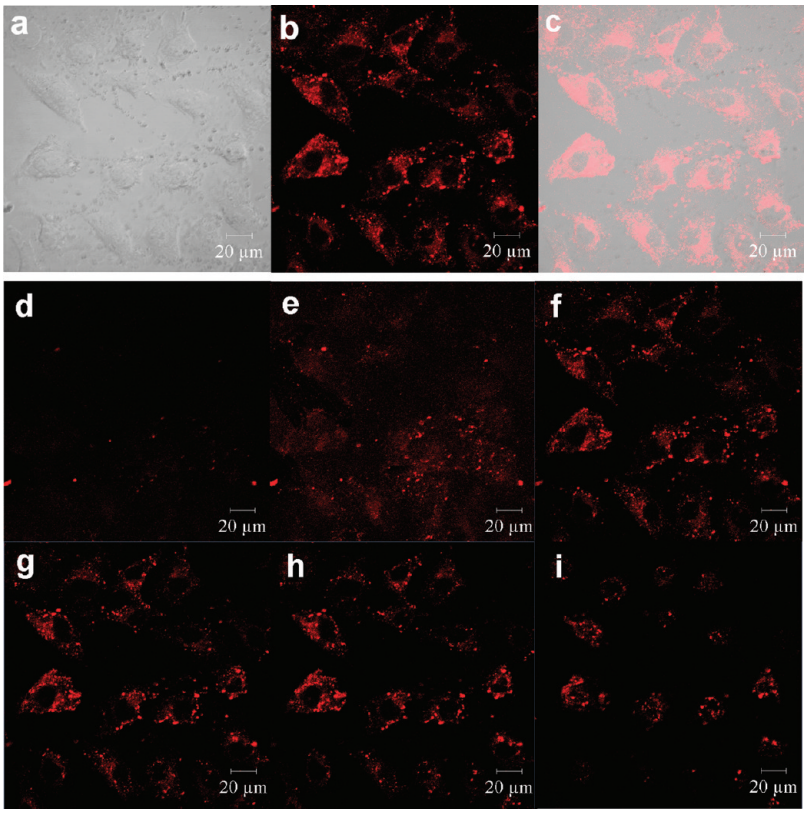

Figure 6. (a) Bright-field, (b) confocal fluorescent, and (c) overlay images of HeLa cells labeled with CS-QD hybrid nanospheres. (d−i) The cut-sections of HeLa cells in image a from top to bottom.

period of a week at room temperature, while the fluorescence of 3-MPA-coated QDs drops rapidly in aqueous medium, as show in Figure 4d,e. Apparently, that protection provided by the chitosan matrices is sufficient enough to prevent any photobleaching to QDs. In addition, the CS-QD hybrid nanospheres are stable in cell culture medium for several weeks (see Figure S2 in the Supporting Information). Therefore, we can consider the hybrid nanospheres used as optical bioimaging agents and drug carriers.

Cytotoxicity and Cell Internalization of Hybrid Nanospheres. It is well-known that the nature of QDs toxicity has greatly limited their practical use in biomedical areas.[31] Thus, we design to circumvent the biocompatibility problem by encapsulating QDs using a biocompatible biopolymer nanosphere without sacrificing the optical of QDs. To evaluate biocompatibility and cytotoxicity of the hybrid nanospheres, we conducted in vitro cytotoxicity tests against cervical cancer cell line HeLa. Figure 5 shows cell viability data obtained from empty CS nanospheres and CS-QD hybrid nanospheres at different concentrations. No cytotoxicity is observed in the cases of either empty CS nanospheres or CS-QD hybrid nanospheres in tested concentration range, suggesting the CS-QD hybrid nanospheres have good biocompatibility.

Compared with other surface modified QDs,[7,10,12−17] the CS-QD hybrid nanospheres have an obvious advantage in photoluminescence of each hybrid nanosphere because multiple QDs (average 9 QDs) were encapsulated in one single nanosphere and did not aggregate due to the protection from a relatively larger polymer matrix. Therefore, the CS-QD hybrid nanospheres may be used as an excellent probe for real-time optical cell imaging, which could be very desirable for cancer diagnosis and treatment. Here, by taking advantage of the inherited optical characteristics from the encapsulated QDs, the cell internalization and intracellular distribution of the CS-QD hybrid nanospheres were evaluated by confocal laser scanning microscopy (CLSM). The QDs encapsulated in the CS-QD hybrid nanospheres should not affect the structure of CS nanospheres, and hence we can believe that the fate of the hybrid nanospheres is determined by CS nanospheres. Figure 6a−c shows fluorescent, bright-field, and overlay images of HeLa cells incubated with CS-QD hybrid nanospheres for 4 h. From the bright-field images of HeLa cells, one can see that the cells incubated with CS-QD hybrid nanospheres are still well-attached to the glass slide and maintain their normal morphology, which corroborates our conclusion about the good biocompatibility of CS-QD hybrid nanospheres. In the fluorescent image, the hybrid nanospheres illuminate the almost entire cell, rendering the hybrid nanospheres suitable as cell-labeling markers. It is also found that most of bright spots occupy the cytoplasm of the cells and the fluorescent signals are not evenly or randomly distributed in cells. These results together along the punctuate fluorescence patterns exhibited in the cells indicate that the cell internalization of CS-QDs hybrid nanospheres follows an endocytosis uptake mechanism.[32] To exclude the possibility of the nonspecific adsorption of hybrid nanospheres on the cell surface, we washed the cells extensively with PBS buffer at 4 and 37 °C after incubation, and LSCM observation was then acquired. From the optical section images from the top to bottom of HeLa cells incubated with CS-QD hybrid nanospheres (Figure 6d−i), we can see that almost no fluorescent signal occurs on the top and

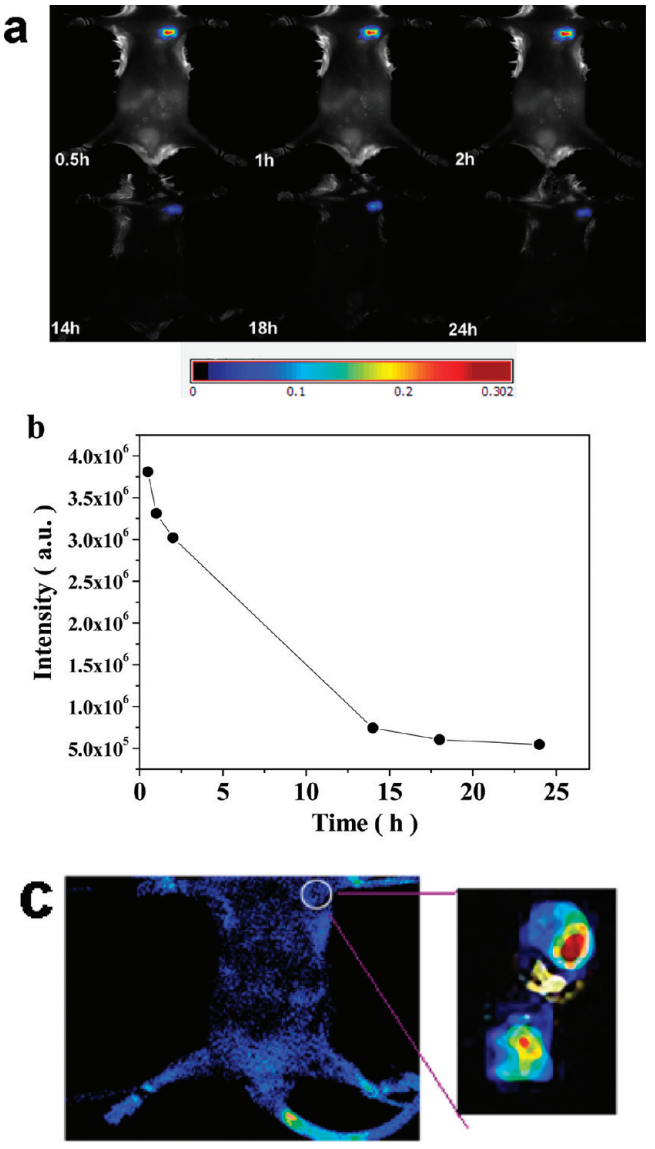

Figure 7. (a) In vivo fluorescence imaging of tumor-bearing mice after intratumoral injection of CS-QD hybrid nanospheres. All images were acquired under the same experiment conditions. The unmixed QD signal is coded in color. (b) The fluorescence intensity for the region-of-tumor was recorded as total photon counts per tumor corresponding to the fluorescence images in part a. (c) Fluorescence imaging of H_{22} tumor-bearing mice 24 h after i.v. injection of CS-QD hybrid nanospheres. Right is the fluorescence imaging of dissected tumor from the mouse in the left.

bottom sections of the cell, especially in the lower left of picture, and strong fluorescent signals come from the middle sections of the cells. These results indicate that fluorescent signals observed come from the hybrid nanospheres which are mainly distributed in the cytoplasm and not those adsorbed at the surface of the cells.

The results from the cell internalization examination in vitro drive us to investigate in vivo tumor imaging of CS-QD hybrid nanospheres in tumor-bearing mice. Time-dependent in vivo fluorescence imaging of CS-QD hybrid nanospheres in tumor-bearing mice was examined by intratumoral (i.t.) and intravenous (i.v.) administration of CS-QDs hybrid nanospheres, respectively. Figure 7a displays the in vivo fluorescence imaging of H_{22} tumor-bearing mice as a time function after intratumoral injection of CS-QD hybrid nanospheres. It can be seen that, within 1 h of postinjection, a strong fluorescence signal is observed in the tumor region and the solid H_{22} tumor can be clearly distinguished from the surrounding normal tissues. During the next 23 h, a steady decrease in the fluorescence intensity at tumor site can be detected. The fluorescence intensity of total photon counts in the tumor as a postinjection time function were calculated, as depicted in Figure 7b. It is apparent that a relatively high concentration of CS-QD hybrid nanospheres in the tumor is maintained within about 2 h postinjection, and then a dramatic decay at tumor site is observed. Nevertheless, the fluorescent signal from the hybrid nanospheres at tumor site can be still identified and is stronger than the autofluorescence of tumor tissue at 24 h postinjection, suggesting that clearance of the hybrid nanospheres at tumor site is not fast and the hybrid spheres can retain in tumor for a long time.

In addition to i.t. administration, we have also carried out bioimaging in the tumor-bearing mice treated by a tail veil injection. It was found that no fluorescent signal was detected in tumor-bearing mice, as shown in Figure 7c. We assumed that this was due to the limited fluorescence penetrability of QDs in deep tissues. To confirm this assumption, the tumor was harvested for isolated imaging at 24 h post i.v. administration. As can be seen in Figure 7d, the characteristic fluorescent signal of CS-QD hybrid nanospheres was observed from H_{22} tumor dissected, indicating that the hybrid nanospheres accumulated preferentially at tumor sites through an enhanced permeability and retention (EPR) effect. According to our previous study,[1,3] empty CS nanospheres could be used as anticancer drug delivery system. It can be believed that CS-QD hybrid nanospheres will be valuable in tumor diagnosis and therapy.

Thus, it is demonstrated that CS-QD hybrid nanospheres can be used for imaging of tumors in tumor-bearing mice. It should also be noted that rapid clearance by the lymphatic drainage system is still the main obstacle for widespread clinical use of nanoparticles in vivo.[33,34] The clearance rate from the tumor is highly dependent on the nanoparticle size and surface charge as reported by Nomura et al.[27] They pointed out that about 70−90% of injected particles remained in tumor after 2 h intratumoral injection for the positively charged particle with the average particle size between 100 to 200 nm. This is good in line with our optical imaging result following i.t. administration. Therefore, CS-QD hybrid nanospheres offer an alternative way to label cancer cells, monitor their cellular internalization patterns, imaging solid tumor locally in the tumor-bearing mice. On the other hand, the tumor accumulation of the hybrid nanospheres was observed via passive targeting at 24 h after i.v. injection. Although the hybrid nanospheres given i.v. do not show fluorescent signal in living imaging as that given i.t. because of the limited fluorescence penetrability of QDs in deep tissues, it is believed that intravenous injection of CS-QD hybrid nanospheres should light up tumor when fluorescence emission of QDs is tuned to near-infrared region. Thus, the CS-QD hybrid nanospheres reported here may be used as a potential prototype system for the realization of cancer diagnosis and therapy.

CONCLUSION

In summary, the CS-QD hybrid nanospheres were successfully prepared by a facile non-solvent-aided counterion complexation

method, and the synthesized CS-QD hybrid nanospheres have desired particle size and QD loading level by varying the ratio among CS, EDTA, and QDs. The obtained hybrid nanospheres were found to have good fluorescent and colloidal stability in physiological environment. Meanwhile, the hybrid nanospheres show remarkable nontoxicity, which makes them suitable well for biomedical application. In vitro cell imaging demonstrated the feasibility of the hybrid nanospheres acting as a labeling agent in cancer-cell imaging. Furthermore, CS-QD hybrid nanospheres can be used for imaging of tumor in tumor-bearing mice via intratumoral administration, which results in a type of hybrid nanosphere that can execute solid tumor cells imaging and cytotoxic agent delivery locally at the tumor site at the same time. In addition, these CS-QD hybrid nanospheres have abundant functional groups on their surface, which can be used for further modification so as to prepare targeting imaging and drug-delivery systems. Thus, the CS-QD hybrid nanospheres will have huge potential for diagnostics and therapeutics of local or regional solid tumors.

■ ASSOCIATED CONTENT

Supporting Information. Additional information and figures (PDF). This material is available free of charge via the Internet at http://pubs.acs.org.

■ AUTHOR INFORMATION

Corresponding Author
*Fax: 86 25 83317761. E-mail: jiangx@nju.edu.cn.

■ ACKNOWLEDGMENT

This study was supported by the Natural Science Foundation of China (51033002, 20874042, and 50625311) and the New Drug Preparation Program of MOST (Grant 2009ZX09503-028).

■ REFERENCES

(1) Hu, Y.; Chen, Q.; Ding, Y.; Li, R.; Jiang, X.; Liu, B. *Adv. Mater.* **2009**, *21*, 1–5.
(2) Guo, J.; Wang, C.; Mao, W.; Yang, W.; Liu, C.; Chen, J. *Nanotechnology* **2008**, *19*, 315605–315612.
(3) Guo, R.; Zhang, L.; Qian, H.; Li, R.; Jiang, X.; Liu, B. *Langmuir* **2010**, *26* (8), 5428–5434.
(4) Liong, M.; Lu, J.; Kovochich, M.; Xia, T.; Ruehm, S. G.; Nel, A. E.; Tamanoi, F.; Zink, J. I. *ACS Nano* **2008**, *2* (5), 889–896.
(5) Chen, H.; Wu, X.; Duan, H.; Wang, Y. A.; Wang, L.; Zhang, M.; Mao, H. *ACS Appl. Mater. Interfaces* **2009**, *1* (10), 2134–2140.
(6) Al-Jamal, W. T.; Al-Jamal, K. T.; Tian, B.; Lacerde, L.; Bomans, P. H.; Frederik, P. M.; Kostarelos, K. *ACS Nano* **2008**, *2* (3), 408–418.
(7) Gao, X.; Cui, Y.; Levenson, R. M.; Chung, L. W. K.; Nie, S. *Nat. Biotechnol.* **2004**, *22* (8), 969–976.
(8) Goto, Y.; Matsuno, R.; Konno, T.; Takai, M.; Ishihara, K. *Biomacromolecules* **2008**, *9*, 3252–3257.
(9) Tan, W. B.; Huang, N.; Zhang, Y. *J. Colloid Interface Sci.* **2007**, *310*, 464–470.
(10) Slevan, S. T.; Patra, P. K.; Ang, C. Y.; Ying, J. Y. *Angew. Chem., Int. Ed.* **2007**, *46*, 2448–2452.
(11) Medintz, I. L.; Uyeda, H. T.; Goldman, E. R.; Mattoussi, H. *Nat. Mater.* **2005**, *4*, 435–446.
(12) Biju, V.; Itoh, T.; Anas, A.; Sujith, A.; Ishikawa, M. *Anal. Bioanal. Chem.* **2008**, *391*, 2469–2495.
(13) Gao, X. L.; Chen, J.; Chen, J. Y.; Wu, B. X.; Chen, H. Z.; Jiang, X. G. *Bioconjugate Chem.* **2008**, *19*, 2189–2195.
(14) Bhang, S. H.; Won, N.; Lee, T.; Jin, H.; Nam, J.; Park, J.; Chung, H.; Park, H.; Sung, Y.; Hahn, S. K.; Kim, B.; Kim, S. *ACS Nano* **2009**, *3* (6), 1389–1398.
(15) Guo, Y.; Shi, D.; Cho, H.; Dong, Z.; Kulkarni, A.; Pauletti, G. M.; Wang, W.; Lian, J.; Liu, W.; Ren, L.; Zhang, Q.; Liu, G. *Adv. Funct. Mater.* **2008**, *18*, 2489–2497.
(16) Kairdolf, B. A.; Mancini, M. C.; Smith, A. M.; Nie, S. *Anal. Chem.* **2008**, *80*, 3029–3034.
(17) Kim, S.; Lim, Y. T.; Soltesz, E. G.; Grand, A. M. D.; Lee, J.; Nakayama, A.; Parker, J. A.; Mihaljevic, T.; Laurence, R. G.; Dor, D. M.; Cohn, L. H.; Bawendi, M. G.; Frangioni, J. V. *Nat. Biotechnol.* **2004**, *22* (1), 93–97.
(18) Sill, K.; Emrick, T. *Chem. Mater.* **2004**, *16* (7), 1240–1243.
(19) Mao, H.; Roy, K.; Troung-Le, V.; Janes, K.; August, T.; Leong, K. *J. Controlled Release* **2001**, *70*, 399–421.
(20) Wang, C.; Wang, L.; Yang, W. *J. Colloid Interface Sci.* **2009**, *333*, 749–756.
(21) Sandros, M. G.; Behrendt, M.; Maysinger, D.; Tabrizian, M. *Adv. Funct. Mater.* **2007**, *17*, 3724–3730.
(22) Qu, L.; Peng, X. *J. Am. Chem. Soc.* **2002**, *124* (9), 2049–2055.
(23) Wang, D.; He, J.; Rosenzweig, N.; Rosenzweig, Z. *Nano Lett.* **2004**, *4* (3), 409–413.
(24) Yu, W. W.; Qu, L.; Guo, W.; Peng, X. *Chem. Mater.* **2003**, *15* (14), 2854–2860.
(25) Smith, A. M.; Duan, H.; Rhyner, M. N.; Ruan, G.; Nie, S. *Phys. Chem. Chem. Phys.* **2006**, *8*, 3895–3903.
(26) Bentolila, L. A.; Ebenstein, Y.; Weiss, S. *J. Nucl. Med.* **2009**, *50* (4), 493–496.
(27) Nomura, T.; Koreeda, N.; Yamashita, F.; Takakura, Y.; Hashida, M. *Pharm. Res.* **1998**, *15*, 128–132.
(28) Schipper, M. L.; Lyer, G.; Koh, A. L.; Cheng, Z.; Ebenstein, Y.; Aharoni, A.; Keren, S.; Chen, X.; Gambhir, S. S. *Small* **2009**, *5* (1), 126–134.
(29) Aldana, J.; Lavelle, N.; Wang, Y.; Peng, X. *J. Am, Chem. Soc.* **2005**, *127*, 2496–2504.
(30) Zhang, H.; Zhou, Z.; Yang, B.; Cao, M. Y. *J. Phys. Chem. B* **2003**, *107* (1), 8–13.
(31) Hauck, T. S.; Anderson, R. E.; Fischer, H. C.; Chan, W. C. W. *Small* **2010**, *6* (1), 138–144.
(32) Verma, A.; Uzun, O.; Hu, Y.; Han, H. S.; Watson, N.; Chen, S.; Irvine, D. J.; Stellacci, F. *Nat. Mater.* **2008**, *7*, 588–595.
(33) Harrington, K. J.; Rowlinson-Busza, G.; Syrigos, K. N.; Uster, P. S.; Vile, R. G.; Stewart, J. S. *Clin. Cancer Res.* **2000**, *6*, 2528–2537.
(34) Bao, A.; Philips, W. T.; Goins, B.; Zheng, X.; Sabour, S.; Natarajan, M.; Ross Woolley, F.; Zavaleta, C.; Otto, R. A. *Int. J. Pharm.* **2006**, *316*, 162–169.